

UNCLASSIFIED

DESIGN AND TESTING OF HARDWARE IMPROVEMENTS OF AN
ACOUSTIC SOUNDER(U) NAVAL POSTGRADUATE SCHOOL MONTEREY
CA W L RICHARDS JUN 85

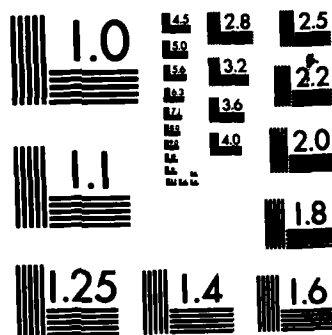
1/1

F/G 28/1

NL

END

LOW MPPA



MICROCOPY RESOLUTION TEST CHART
NATIONAL BUREAU OF STANDARDS-1963-A

2

NAVAL POSTGRADUATE SCHOOL

Monterey, California

AD-A159 672



THESIS

DTIC
ELECTE
OCT 4 1985
S A D

DESIGN AND TESTING OF HARDWARE
IMPROVEMENTS OF AN ACOUSTIC SOUNDER.

by

William L. Richards

June 1985

Thesis Advisor:

D.L. Walters

Approved for public release; distribution unlimited

DTIC FILE COPY

85 10 04 04M

REPORT DOCUMENTATION PAGE		READ INSTRUCTIONS BEFORE COMPLETING FORM
1. REPORT NUMBER	2. GOVT ACCESSION NO. AD A159672	3. RECIPIENT'S CATALOG NUMBER
4. TITLE (and Subtitle) DESIGN AND TESTING OF HARDWARE IMPROVEMENTS OF AN ACOUSTIC SOUNDER		5. TYPE OF REPORT & PERIOD COVERED Master's Thesis June 1985
		6. PERFORMING ORG. REPORT NUMBER
7. AUTHOR(s) William L. Richards		8. CONTRACT OR GRANT NUMBER(s)
9. PERFORMING ORGANIZATION NAME AND ADDRESS Naval Postgraduate School Monterey, California 93943-5100		10. PROGRAM ELEMENT, PROJECT, TASK AREA & WORK UNIT NUMBERS
11. CONTROLLING OFFICE NAME AND ADDRESS Naval Postgraduate School Monterey, California 93943-5100		12. REPORT DATE June 1985
		13. NUMBER OF PAGES 51
14. MONITORING AGENCY NAME & ADDRESS (if different from Controlling Office)		15. SECURITY CLASS. (of this report) Unclassified
		15a. DECLASSIFICATION/DOWNGRADING SCHEDULE
16. DISTRIBUTION STATEMENT (of this Report) Approved for public release; distribution unlimited		
17. DISTRIBUTION STATEMENT (of the abstract entered in Block 20, if different from Report)		
18. SUPPLEMENTARY NOTES		
19. KEY WORDS (Continue on reverse side if necessary and identify by block number) Laser Acoustic Sonuder Horn		
20. ABSTRACT (Continue on reverse side if necessary and identify by block number) Acoustic sounders have proven to be excellent tools in probing the fine dynamic structure of the atmosphere. Commercial instruments, such as the Aeroviroment model #300 acoustic sounder, are qualitative devices and do not operate well at ranges beyond 500 meters. This project centered on two hardware improvements designed to help increase the range of the acoustic sounder to over one thousand meters. The de- velopments include the design and testing of an improved		

transmission horn for the transducer.

Approved for public release; distribution unlimited

Design and Testing of Hardware Improvements
of an Acoustic Sounder

by

William L. Richards
Lieutenant, United States Navy
B.S., United States Naval Academy, 1977



Submitted in partial fulfillment of
requirements for the degree of

MASTER OF SCIENCE IN PHYSICS

from the

NAVAL POSTGRADUATE SCHOOL
June 1985

Author:

William L. Richards

William Richards

Approved by:

Donald Walters

Donald Walters, Thesis Advisor

Alan B. Coppens

Alan Coppens, Second Reader

Gordon Schacher

Gordon Schacher, Chairman, Department of Physics

John Dyer

John Dyer, Dean of Science and Engineering

Accession For	
NTIS	CRA&I <input checked="" type="checkbox"/>
DTIC	TAB <input type="checkbox"/>
Unannounced	<input type="checkbox"/>
Justification	
By	
Distribution	
Availability Codes	
Dist	Avail and/or Special
A1	

ABSTRACT

Acoustic sounders have proven to be excellent tools in probing the fine dynamic structure of the atmosphere. Commercial instruments, such as the Aerovironment model #300 acoustic sounder, are qualitative devices and do not operate well at ranges beyond five hundred meters. This project centered on two hardware improvements designed to help increase the range of the acoustic sounder to over one thousand meters. The developments include the design and testing of an improved transmission horn for the transducer.

TABLE OF CONTENTS

I.	INTRODUCTION	7
II.	PROBLEM DESCRIPTION	8
	A. BACKGROUND	8
	B. THEORY	10
	1. General Horn Theory	10
	2. Transmission Factor	14
	C. DESIGN	17
	1. The Exponential Horn	17
	2. The Catenoidal Horn	24
III.	TESTING AND RESULTS	28
	A. EXPERIMENTAL PROCEDURE	28
	1. General	28
	2. Equipment Description	29
	3. Procedure	31
	B. RESULTS	34
	C. CONCLUSIONS AND RECOMMENDATIONS	39
	APPENDIX A: DESIGN COMPUTER PROGRAMS	45
	APPENDIX B: DIMENSIONS OF THE DESIGN HORNS	47
	APPENDIX C: DATA	48
	LIST OF REFERENCES	50
	INITIAL DISTRIBUTION LIST	51

LIST OF FIGURES

1.	Block Diagram of the Acoustic Sounder.	9
2.	General Horn Diagram	11
3.	Graph of Transmission Factor versus Frequency for a Conical Horn	16
4.	Graph of Transmission Factor versus Frequency for an Exponential Horn.	18
5.	Graph of Transmission Factor versus Frequency for a Catenoidal Horn	19
6.	Diagram of the Conical Horn	21
7.	Engineering Drawing of the Exponential Design	23
8.	Engineering drawing of the Catenoidal Design	27
9.	Intensity Level Testing Equipment Setup	30
10.	Beam Pattern Testing Equipment Setup	32
11.	Graph of the Reciprocal of the Square Root of Intensity versus Distance for the Conical Horn	36
12.	Graph of the Reciprocal of the Square Root of Intensity versus Distance for the Exponential Horn	37
13.	Graph of the Reciprocal of the Square Root of Intensity versus Distance for the Catenoidal Horn	38
14.	Beam Pattern of the Conical Horn at 1 Meter	40
15.	Beam Pattern of the Exponential Horn at 1 Meter	41
16.	Beam Pattern of the Catenoidal Horn at 1 Meter	42
17.	Beam Pattern of the Driver at 1 Meter.	43

I. INTRODUCTION

The application of lasers in military communications and weapons systems accentuate the need for instruments capable of measuring the fine dynamic structure of the atmosphere. One of the most useful tools available for the probing of the atmosphere is the acoustic sounder. Commercial grade acoustic sounders, such as the Aerovironment model #300 cannot collect atmospheric data with the quality needed for laser propagation research. The usable range of the Aerovironment model #300 acoustic sounder is less than 500 meters. Many laser systems need atmospheric information at altitudes of 1 to 2 kilometers and higher. The objective of this thesis was to upgrade an existing acoustic sounder to increase the range and improve the quality of the receiver-processor. A serious deficiency of the Aerovironment model #300 is the poor coupling of the acoustic transducer to the feedhorn. This thesis involved a complete redesign and experimental test of the transducer feedhorn using two different horn styles as well as making the horn removable and easily changeable. Additional

Keywords: Experimental data; Charts; Equations

II. PROBLEM DESCRIPTION

A. BACKGROUND

The Aerovironment model #300, described in Reference 1, is an acoustic sounder or acoustic radar. Figure 1 shows the monostatic device which is used for analyzing the structure of the atmosphere from a minimum of twenty meters to a maximum of about five hundred meters above ground level. The echo returns of interest, produced by turbulent atmospheric density fluctuations, are recorded on chart paper that provides a continuous record of the intensity of the echo returns as a function of height and time. The sounder as presently configured, can operate over a twenty eight day period thereby recording long-term atmospheric structure.

The active element in the antenna assembly is the 1.6 kilohertz transducer, which functions as a loudspeaker and receive antenna. This transducer signal is coupled through a conical horn to a one meter parabolic dish positioned by braces so the horn is at the focal point of the dish. It was suspected that this conical horn could be replaced by a more efficient design in order to increase the performance of the system and extend the maximum range to about 1 kilometer. This thesis research involved the design, fabrication, and

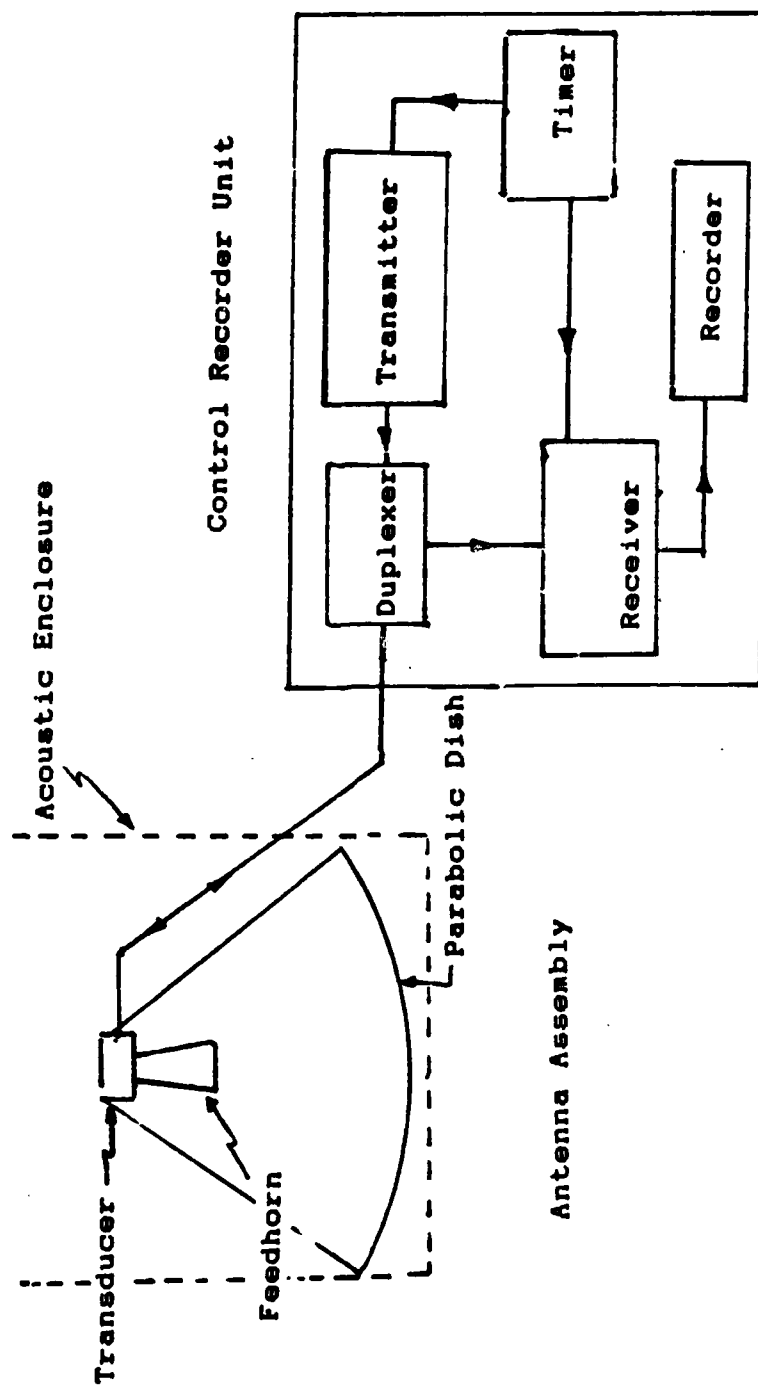


Figure 1. Block Diagram of the Acoustic Sounder

measurements of an exponential and catenoidal horn. A factor of eight improvement in radiated acoustic energy was expected for both horn designs compared to the existing conical horn.

B. THEORY

1. General Horn Theory

Merhaut [Ref. 2] describes the transmission horn as an acoustic transformer. It attempts to match the impedance difference between a small area diaphragm and the free atmosphere. To develop a one-dimensional wave equation, the axis of the horn is assumed to be a straight line coincident with the x axis. The walls of the horn are assumed to be perfectly rigid. To simplify the mathematical development, a plane wave, with wavefronts perpendicular to the x axis, is assumed to propagate through the horn. The cross section of the horn, S , is a function of x (Fig. 2). This functional dependence is different for each specific horn design. It is also assumed, for ease of solution, that the throat diameter of the horn is small compared to the wavelength.

The equation of continuity can be obtained as follows: The increase of mass per unit time at a cross section situated at a given position, x , is the difference of the mass which flows in unit time into the element Δx through the cross section S with a velocity v and the mass which flows per unit time out of the element Δx through the cross section S^* with the velocity v^* at the

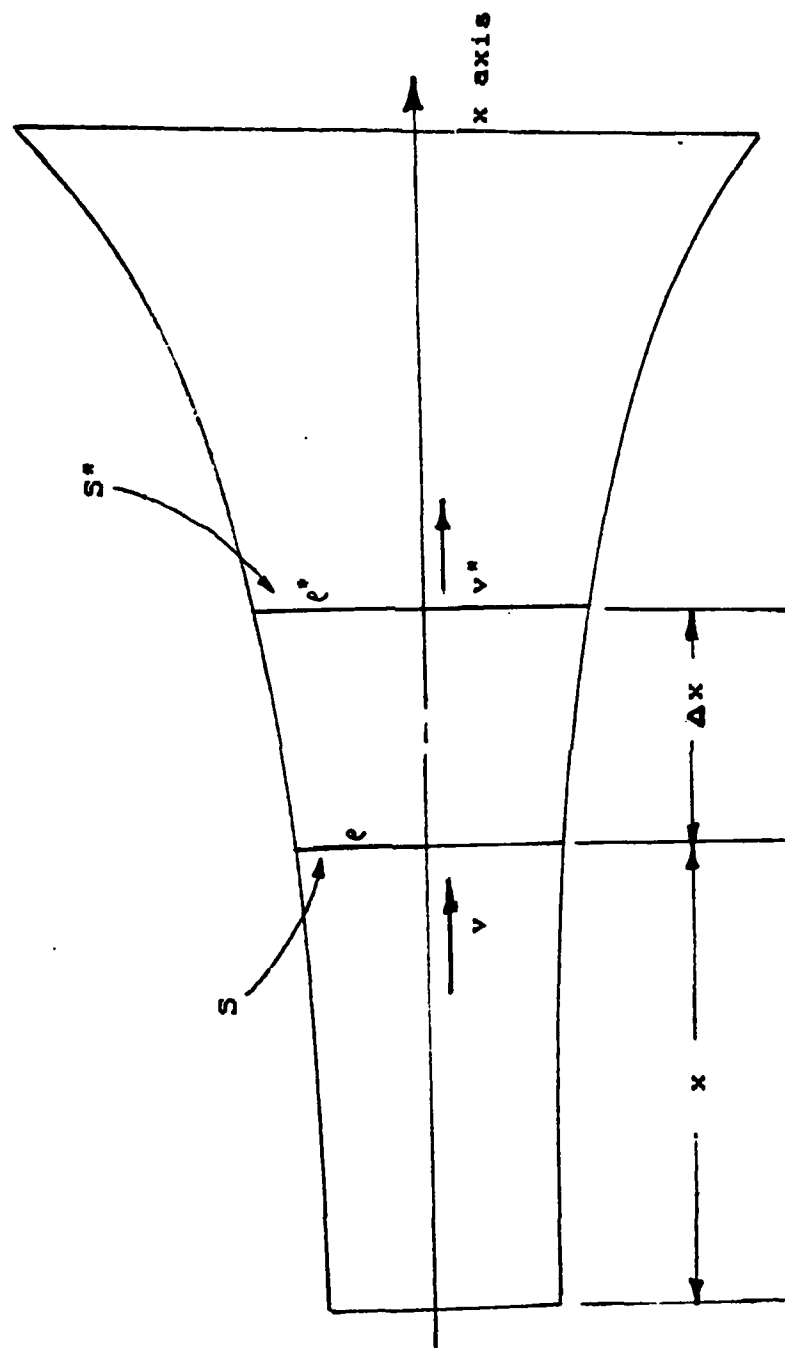


Figure 2. General Horn Diagram

position $x + \Delta x$. The mass difference is

$$Sv\rho - S^*v^*\rho^* \quad , (1)$$

where ρ is the density. In the limit, as Δx approaches zero

$$\lim_{\Delta x \rightarrow 0} (Sv\rho - S^*v^*\rho^*) = - \frac{\partial(Sv\rho)}{\partial x} \quad . (2)$$

This mass will cause an increase per unit time of the density in an element, the volume of which is $S dx$. Thus

$$S dx = - \frac{\partial(Sv\rho)}{\partial x} dx \quad . (3)$$

Neglecting the changes of ρ along x , since they are small compared with the average value, the equation of continuity is obtained.

$$S \frac{\partial \rho}{\partial x} + \rho \frac{\partial(Sv)}{\partial x} = 0 \quad . (4)$$

This is the equation of continuity for a horn of cross section that varies as $S = f(x)$.

The velocity potential, defined as a scalar that has its gradient equal to the particle velocity, ($\text{grad } \phi = v$) can be substituted into Equation 4 above to yield

$$- \frac{1}{S} \frac{\partial}{\partial x} \left(S \frac{\partial \phi}{\partial x} \right) = - \frac{1}{\rho} \frac{\partial \rho}{\partial t} \quad . (5)$$

Carrying out the partial differentiation of the product in brackets in Equation 5 gives

$$\frac{\partial^2 \phi}{\partial x^2} + \frac{1}{S} \frac{dS}{dx} \frac{\partial \phi}{\partial x} = - \frac{1}{\rho} \frac{\partial \rho}{\partial t} \quad . (6)$$

Substituting Poisson's equation as the general solution for

a wave equation (which is applicable also to horns),

$$\frac{1}{c} \frac{\partial p}{\partial t} = \frac{1}{c_0^2} \frac{\partial^2 \phi}{\partial t^2} \quad , (7)$$

into Equation 6 gives

$$\frac{\partial^2 \phi}{\partial x^2} + \frac{1}{S} \frac{dS}{dx} \frac{\partial \phi}{\partial x} = \frac{1}{c_0^2} \frac{\partial^2 \phi}{\partial t^2} \quad . (8)$$

This wave equation for horns is sometimes called the Webster Equation. Since

$$1/S(dS/dx) = d/dx(\ln S),$$

it is possible to write the Webster Equation as

$$\frac{\partial^2 \phi}{\partial x^2} + \frac{\partial \phi}{\partial x} \frac{d}{dx} (\ln S) - \frac{1}{c_0^2} \frac{\partial^2 \phi}{\partial t^2} = 0 \quad . (9)$$

The solution of this equation depends upon the shape of the horn which determines the function $S = f(x)$. In the case of the conical horn, the function S varies according to the equation

$$S = S_0 x^2 \quad . (10)$$

A straight exponential horn of cross section S perpendicular to the x axis is given by the equation

$$S = S_0 e^{ax} \quad . (11)$$

The a here is called the flare constant. Obviously, a determines the shape of the horn. The greater a becomes, the greater the flare of the horn. When $a = 0$ (no flare) the equation becomes that of a straight cylindrical tube. A

hyperbolic or catenoidal horn is given by the equation

$$S = S_0 \cosh^2 (x/h) \quad . \quad (12)$$

In Equation 12, h is a scale factor measuring how slowly the catenoidal horn flares out.

2. Transmission Factor

A good measure of the radiating efficiency of a transmission horn is its corresponding transmission factor. The transmission factor is defined as the ratio of the power radiated out of a given horn to the power radiated by the same diaphragm, moving at the same velocity, into a cylindrical tube of infinite length, having the same cross-sectional area as the small end of the horn. The general equation for the transmission factor as presented in Morse [Ref. 3] is

$$T = \frac{2 \Pi}{S_0 \rho c u_0^2} = \frac{R}{\rho c} \quad , \quad (13)$$

where

Π = power radiated out of the horn,

S = throat cross-sectional area,

ρc = characteristic acoustic resistance
(415 kg/m² sec for air at standard
temperature and pressure),

u_0 = particle velocity at the throat,

R = acoustic resistance.

This ratio is not, strictly speaking, an efficiency, but rather a ratio of actual power radiated out of a horn to the power radiated for a convenient reference case.

Consequently, the transmission factor may exceed unity (as in the case of the catenoidal horn). In general, however,

the transmission factor varies between zero and one. When it is small the the diaphragm will have to vibrate with large amplitude to radiate significant power.

The horn on the premodified acoustic sounder transducer assembly was a conical horn. The equation of the transmission factor for a conical horn, again from Morse, is

$$T_c = \frac{(2 \pi f x_0)^2}{c^2 + (2 \pi f x_0)^2}, \quad (14)$$

where f = transmit frequency,
 x_0 = distance from the throat to the apex of the cone,
 c = speed of sound in free space.

The larger the frequency, the closer the transmission factor for the conical horn approaches unity (Fig. 3). The calculated transmission factor using Equation 11 and the measured distance to the apex of 1.27 cm. at a frequency of 1.6 kilohertz for the conical horn was 0.128. Clearly this figure showed that the conical horn on the premodified transducer was a poor design choice for the acoustic sounder. Increasing the transmission coefficient will improve the efficiency of the transmitter horn.

An efficient horn possibility is the exponential horn. The transmission factor for the exponential horn is given by Morse as

$$T_e = \sqrt{1 - (f_0/f)^2}, \quad (15)$$

where f_0 = cutoff frequency.

This frequency f_0 is called the cutoff frequency because

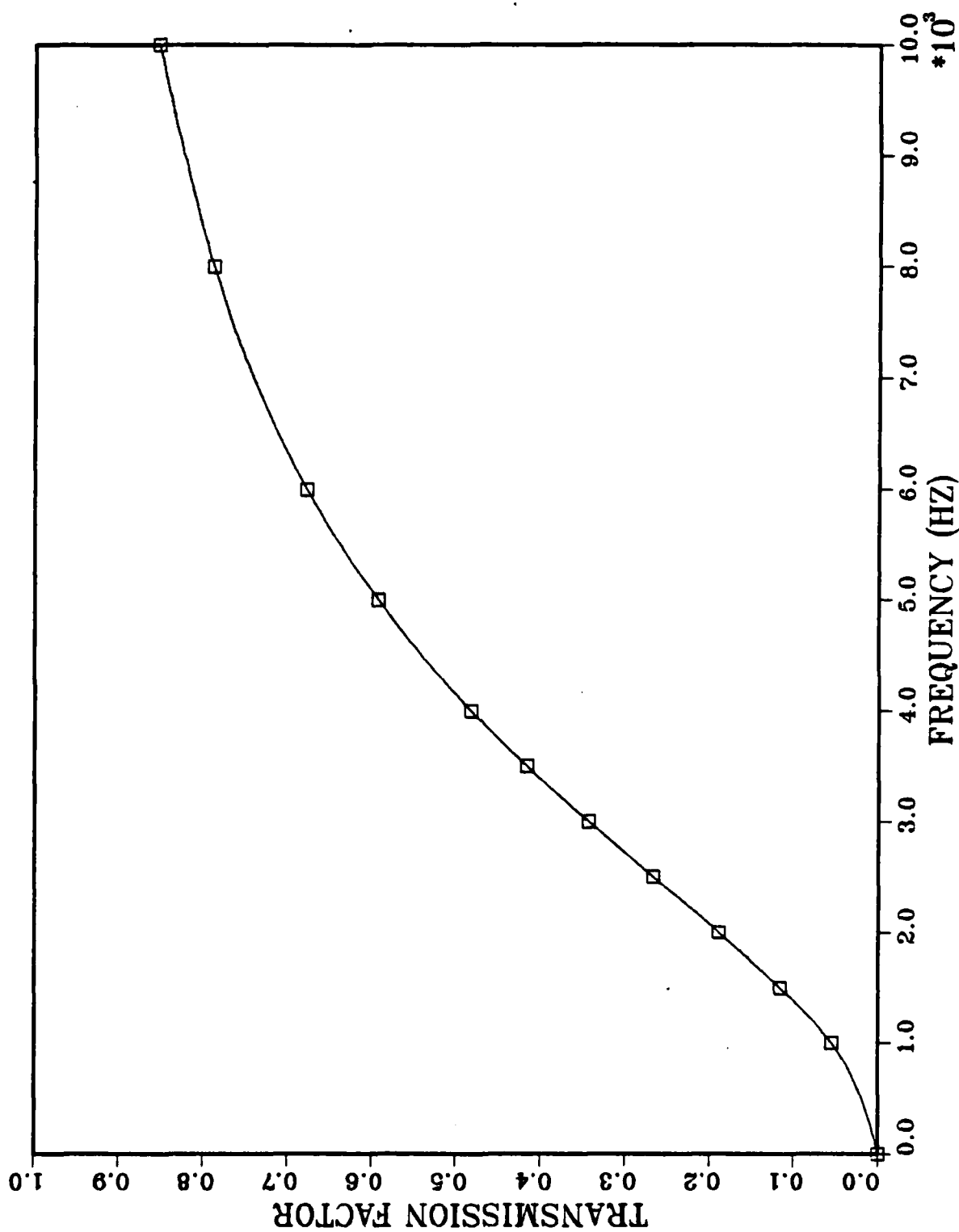


Figure 3. Graph of Transmission Factor versus Frequency for a Conical Horn.

for frequencies lower than f_0 , power will not be transmitted down the horn. The impedance at all positions along the horn will be completely reactive. Above the cutoff frequency, the transmission factor rises sharply with frequency for the exponential horn (Fig. 4). As Equation 15 clearly shows, choosing the correct cutoff frequency for the exponential horn is crucial to a high transmission factor.

A hyperbolic or catenoidal horn offers a second possibility to raise the transmission factor of the transducer. The equation from Reference 4 for the transmission factor of a catenoidal horn is

$$T_h = \frac{1}{\sqrt{1 - (f_0/f)^2}} \quad . \quad (16)$$

This is the inverse of the exponential horn transmission factor, and decreases with the transmission factor approaching unity as the frequency approaches infinity (Fig. 5). With the catenoidal horn design it is a distinct possibility that a transmission factor of greater than unity can be obtained.

C. DESIGN

1. The Exponential Horn

Since the transmission factor of the present conical design proved to be 0.128 an exponential horn was designed. To get an efficient design for the exponential horn an accurate cutoff frequency must be established for the 1.6 kilohertz centerline acoustic frequency of the transducer.

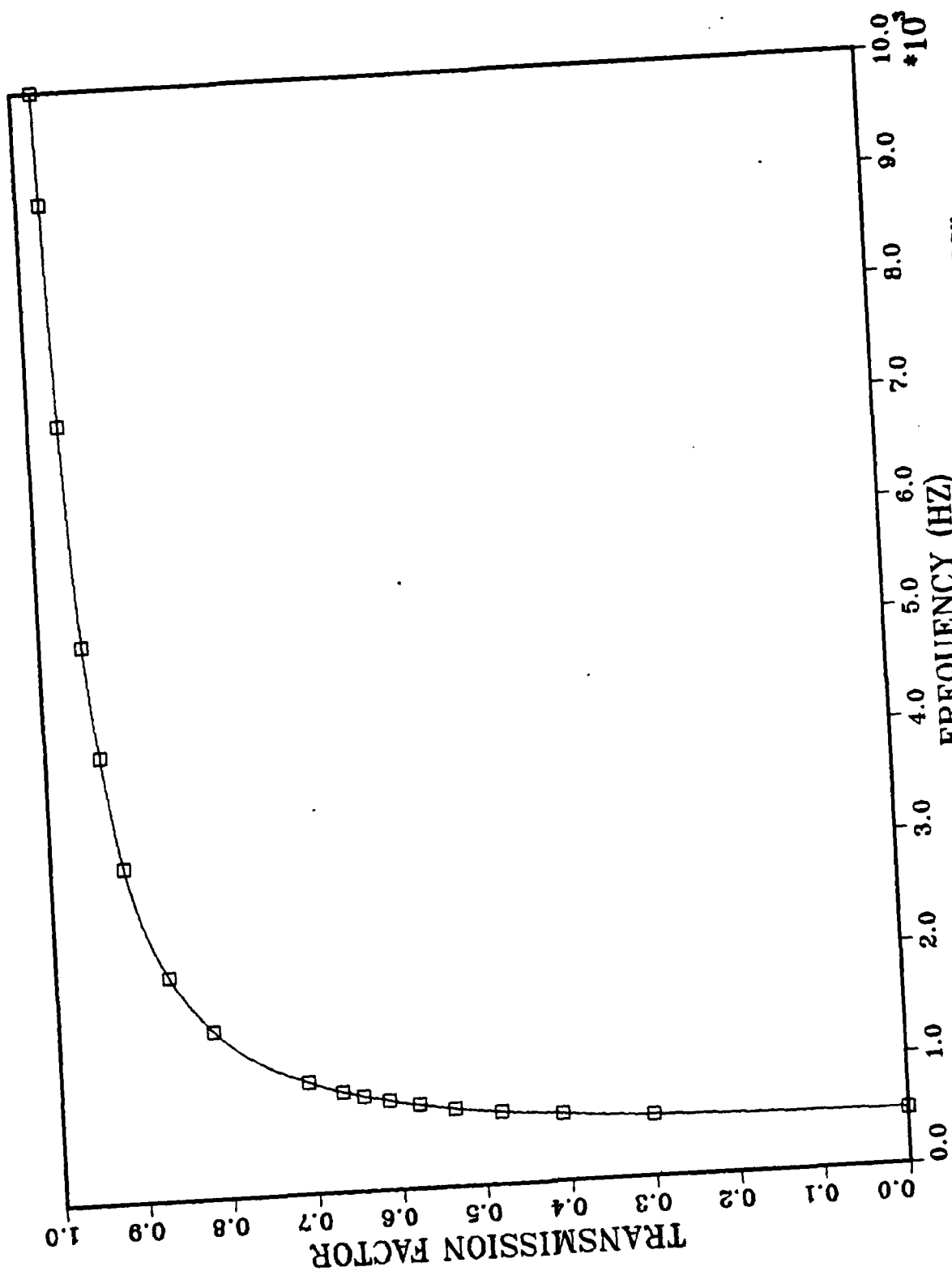


Figure 4. Graph of Transmission Factor versus Frequency for an Exponential Horn.

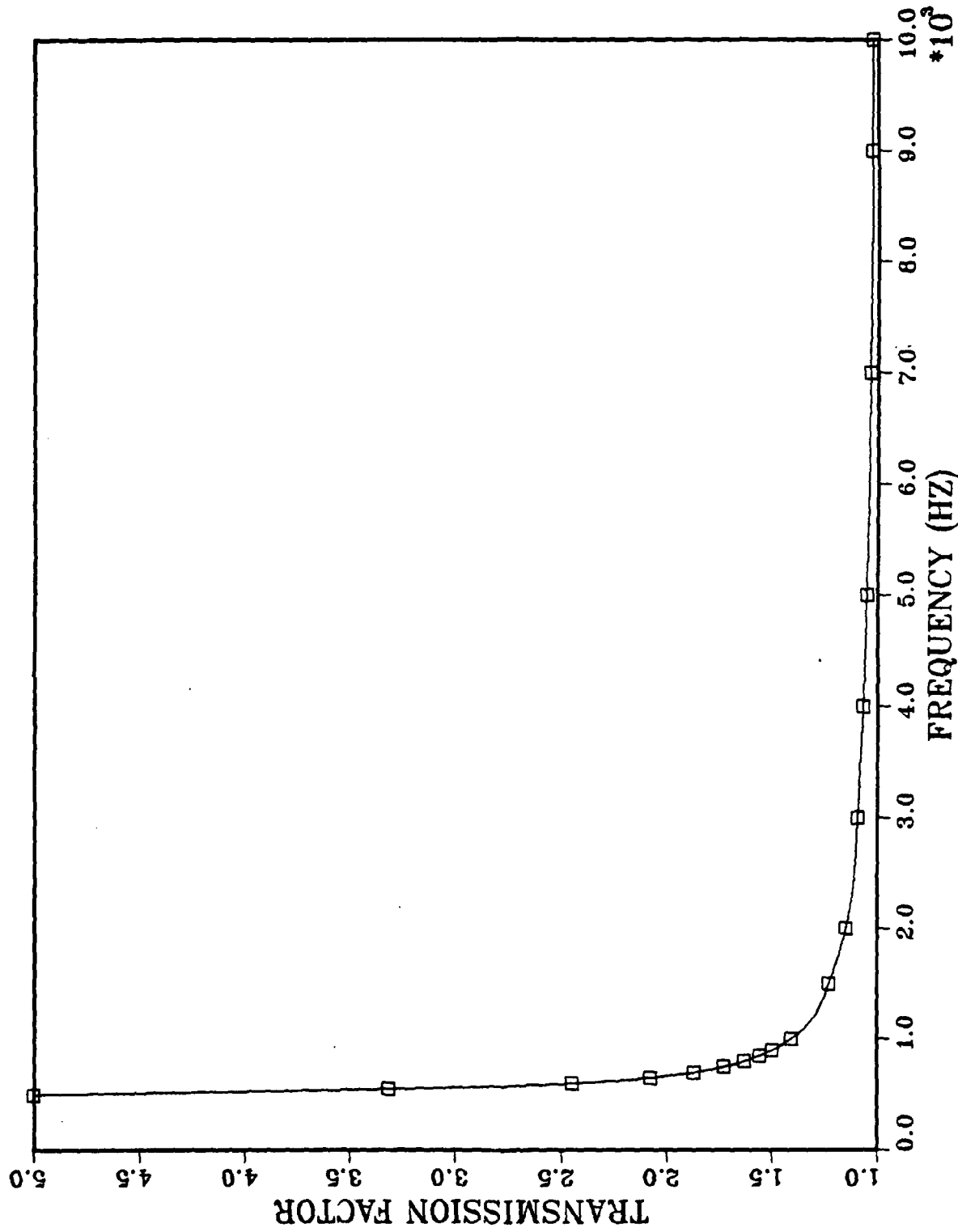


Figure 5. Graph of Transmission Factor versus Frequency for a Catenoidal Horn.

The easiest way to determine a crude approximation for the cutoff frequency was to determine the cutoff frequency of the present conical horn mouth circumference and apply it as the starting point for the exponential design. The equation for cutoff frequency is directly derived from the solution to Webster's equation (Eq. 9) using Equation 11 as the standard function for the exponential horn. In terms of the mouth diameter D_m , the cutoff frequency is

$$f_0 = c_0 / \pi(D_m) \quad (17)$$

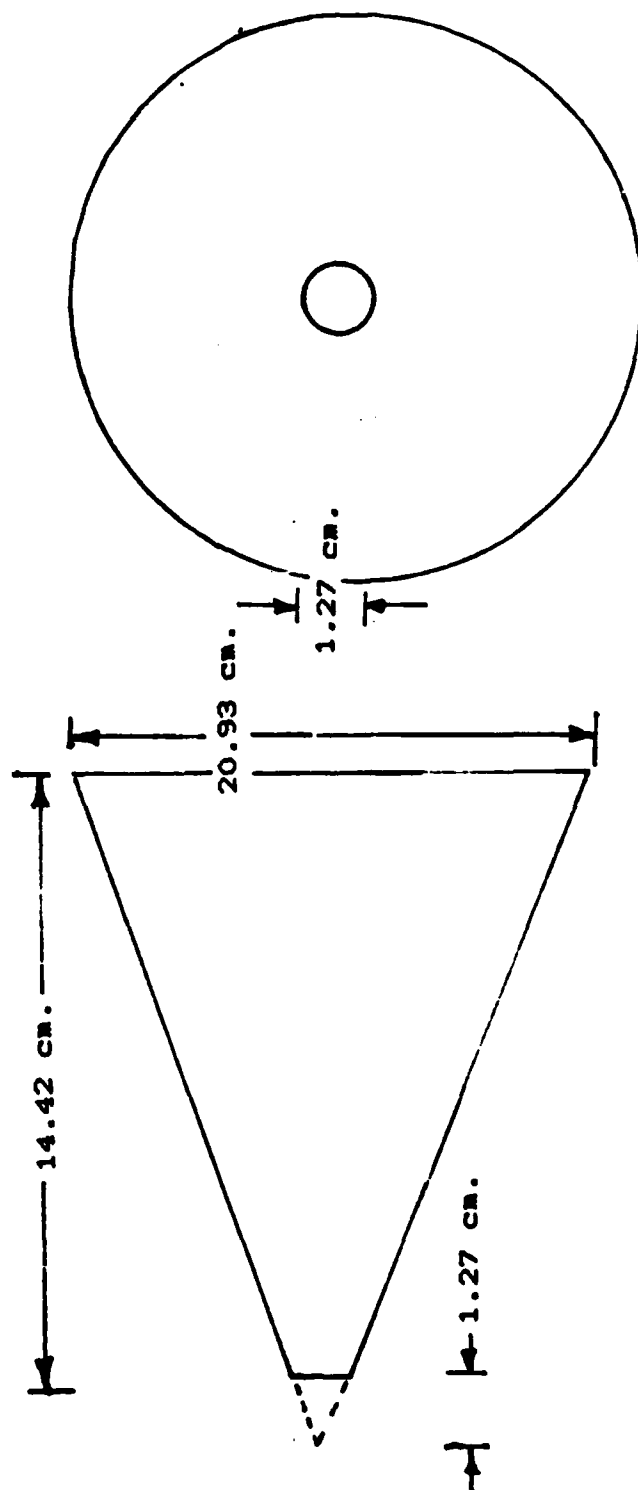
where c_0 = speed of sound in air at standard temperature and pressure. Using the conical horn mouth diameter of 20.93 cm, as detailed in Figure 6, yielded a cutoff frequency of 500 Hz. The cutoff frequency of 500 Hz was used for all future calculations including the design of the catenoidal horns.

Once the cutoff frequency was chosen, the next parameter to be determined in the design of the exponential horn was the flare constant, m . The flare constant for exponential horns can be expressed as

$$m = 4 \pi v_0 / c_0. \quad (18)$$

Using the cutoff frequency calculated above the flare constant is 18.98 m^{-1} .

Now that the design constants were determined the actual calculation of the dimensions of the exponential horn could begin. Equation 11 is the determining equation for the exponential horn family and was used as the basis for a computer design program for the horn. This program is listed



(not to scale)

Figure 6. Diagram of the Conical Horn

as Appendix A. For good design, the mouth of the horn should have a circumference large enough so that the radiation impedance is nearly resistive over the desired frequency range. In this case, the anticipated doppler due to vertical motion in the atmosphere is small, plus or minus 20 Hz at 1600 Hz. According to Beranek [Ref. 5], this is true when the circumference of the mouth divided by the wavelength of the lowest transmitted wave is greater than one. Using this rule, the length of the exponential horn can be determined. Using the wavelength of the transmitted frequency, namely 20.69 cm. as a limiting value, the corresponding length (x) is 18 cm. Therefore, the horn must be greater than eighteen centimeters in length to match the impedance correctly. For ease of manufacture, the exponential horn length was chosen to be twenty centimeters. An engineering drawing of the design was made to facilitate manufacture and a flange was built into the base of the horn (near the throat) to aid in ease of attachment and removal. This drawing appears as Figure 7. The new transmission factor was calculated for this exponential design using Equation 15 and found to be 0.902. This is a marked improvement over the conical horn's 0.128 transmission factor.

The exponential horn was built from an aluminum mold turned on a lathe to the dimensions given for the inside diameter in Appendix B. A fiberglass resin was then applied to the mold to form the 0.4 centimeter shell of the

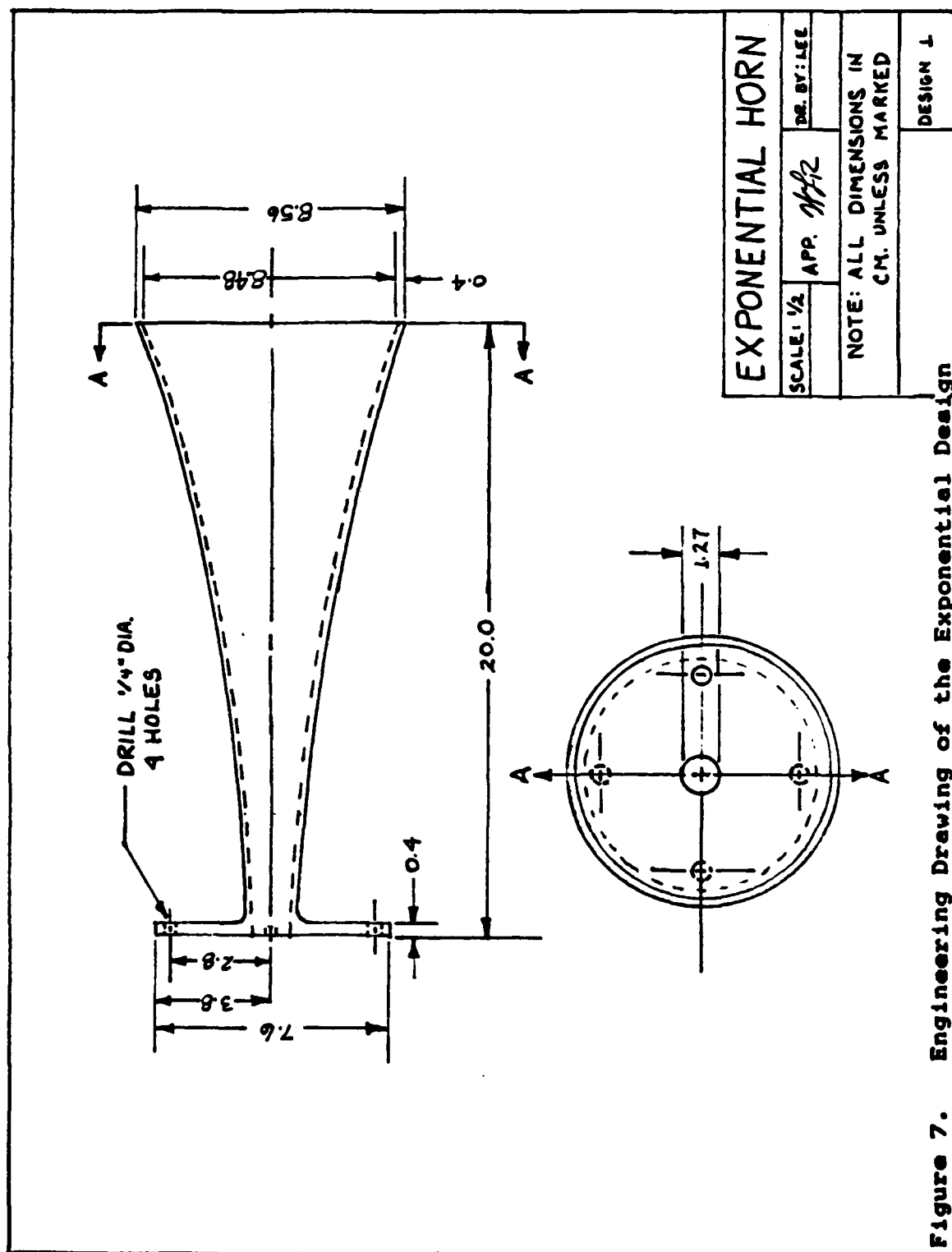


Figure 7. Engineering Drawing of the Exponential Design

exponential horn. The material from which the horn is constructed is very important. If the side walls of the horn resonate mechanically at one or more frequencies in the range of operation a "dip" in the power curve (and hence a loss in the transmission factor) will occur. Undamped thin metal, such as aluminum, is the least desirable material because the horn will resonate at moderate frequencies such as the 1.6 kilohertz frequency of this transducer. Heavy metals, covered on the outside with a thick mastic material so that the mechanical resonances are damped, are much better, but are difficult to manufacture. Fiberglass was chosen as the most acceptable compromise to the problem of ease of manufacture versus horn mechanical resonance.

2. The Catenoidal Horn

Another design choice in the attempt to raise the transmission factor of the transducer feedhorn is the catenoidal or hyperbolic design. There are two definite advantages to the catenoidal horn design. First, the transmission factor can be raised to a level greater than one (as it was in this design), and second the catenoid design approaches a perfect cylindrical tube at the throat. This allows one to tune the resonate frequency of the horn if it is significant by adjusting the length of this cylidrical section.

Again, as in the exponential design, the catenoidal horn requires a careful choice of the cutoff frequency. The solution to Webster's equation (Eq. 9) using Equation 12 as the standard function for a hyperbolic horn yields a cutoff frequency remarkably close to 500 Hz. While the cutoff frequency of the catenoidal family is usually slightly higher than the corresponding exponential design, 500 Hz was kept as the baseline cutoff frequency.

The next parameter to be chosen in the design is the hyperbolic flare constant, h . The hyperbolic flare constant can be expressed as

$$h = c / (2 \pi f_0). \quad (19)$$

Using the cutoff frequency of 500 Hz and the speed of sound at standard temperature and pressure as 331.6 m/s, the hyperbolic flare constant is 0.1054 m^{-1} .

With the design components chosen, the calculation of the dimensions of the catenoidal horn could now be made. Again, as in the exponential design, a computer design program, introduced as Appendix A, was written to aid in the calculation of the inner wall dimensions of the horn. Equation 12 was used as the basis of this computer program with the hyperbolic function converted to its exponential analog for programming ease. The differences between the hyperbolic and exponential functions are so small that the 0.01 centimeter machining accuracy of the milling lathe producing the horn mold was the primary uncertainty. To

maximize the horn resonance an odd quarter wavelength multiple was chosen. Since the wavelength of the 1.6 kilohertz frequency is 20.69 centimeters, a length of $5/4$ of a wavelength was chosen. This distance (x) from the throat is 25.86 centimeters which was rounded to 25 centimeters for ease in manufacture of the mold. As in the case of the exponential horn, an engineering drawing was made of the design and appears as Figure 8. To aid in the attachment and removal of the horn, a flange was designed into the throat of the horn. The transmission factor for this catenoidal horn using Equation 16 was found to be a design 1.052. The design efficiency is a full eight times greater than the 0.128 transmission factor of the existing conical horn.

The catenoidal horn was constructed in a manner similar to the exponential horn. An aluminum mold was crafted on a machining lathe from the dimensions in Appendix B. Next a layer of gel coat was applied over a silicon mold release onto which the fiberglass resin was formed. The resulting 0.4 centimeter thick fiberglass horn was found to be rigid and quite non-resonating.

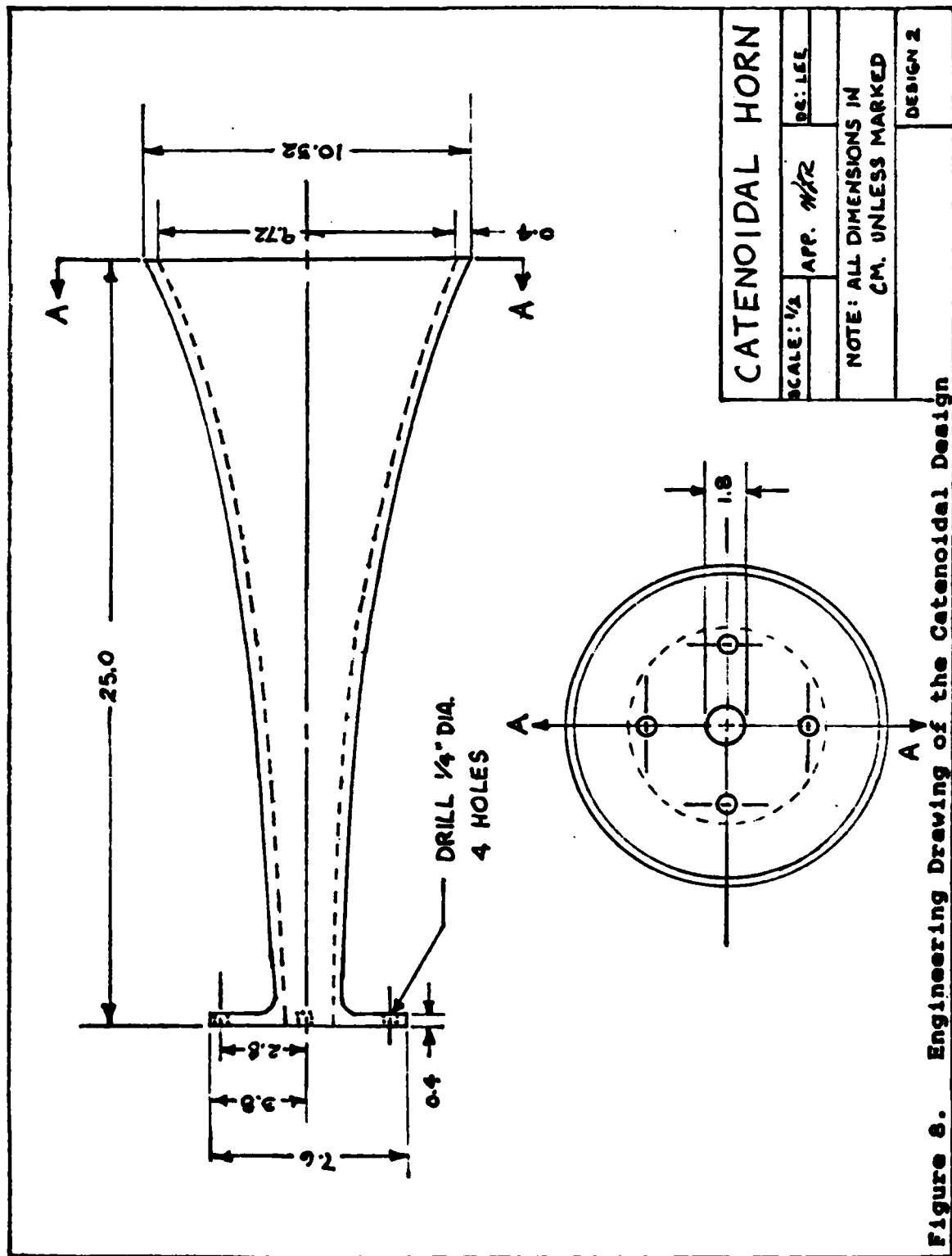


Figure 8. Engineering Drawing of the Catenoidal Design

III. TESTING AND RESULTS

A. EXPERIMENTAL PROCEDURE

1. General

After completion of the design and manufacture of the two test horns, the next step was to test the acoustic output to see if the designs achieved their theoretical expectations. To utilize the horns with a parabolic antenna it was necessary to find the acoustic focal point of each, test their power output, determine the corresponding beam patterns, and finally, compare the new design characteristics with the original conical horn output characteristics.

Since there is active and continuing research on various acoustic propagation projects at the Naval Postgraduate School, much of the testing equipment for this experiment was readily available. Each experiment was conducted in the anechoic chamber in the basement of Spanagel Hall to reduce the ambient background noise. The exponential, catenoidal, and conical horns as well as the driver itself were tested. The same driver for each horn design was used. The bare driver, with no horn attached, was also tested to be used as the control for the experiment.

2. Equipment Description

To determine the acoustic center and to get an accurate angular output power distribution for each horn, a simple method of testing was devised. Every test run was the same for all horn designs as well as the original conical horn and the driver (with no horn attached). The transducer/horn assembly was suspended from the ceiling of the anechoic chamber by a small metal rod. Pointed directly at the aligned transducer diaphragm was a calibrated 2.54 cm. diameter microphone. The Altec 688A microphone was suspended at exactly the same height as the transducer on a moveable rod so that the distance between the diaphragm and the microphone could be decreased after each reading. The microphone was then connected through a HP 462A preamplifier and amplifier system to a sonometer and voltage measuring device. Intensity readings could be taken in both decibels and millivolts. The transducer was driven by a separate HP 435A amplifier and signal generator. Figure 9 details the apparatus for this portion of the experimental trials. The microphone could then be moved inward along the acoustic axis of the horn/driver system and accurate measurements of the intensity level could be made at predetermined distances.

The apparatus required to obtain the beam patterns for the three horns was a bit more difficult to devise. Instead of the microphone moving in relation to the

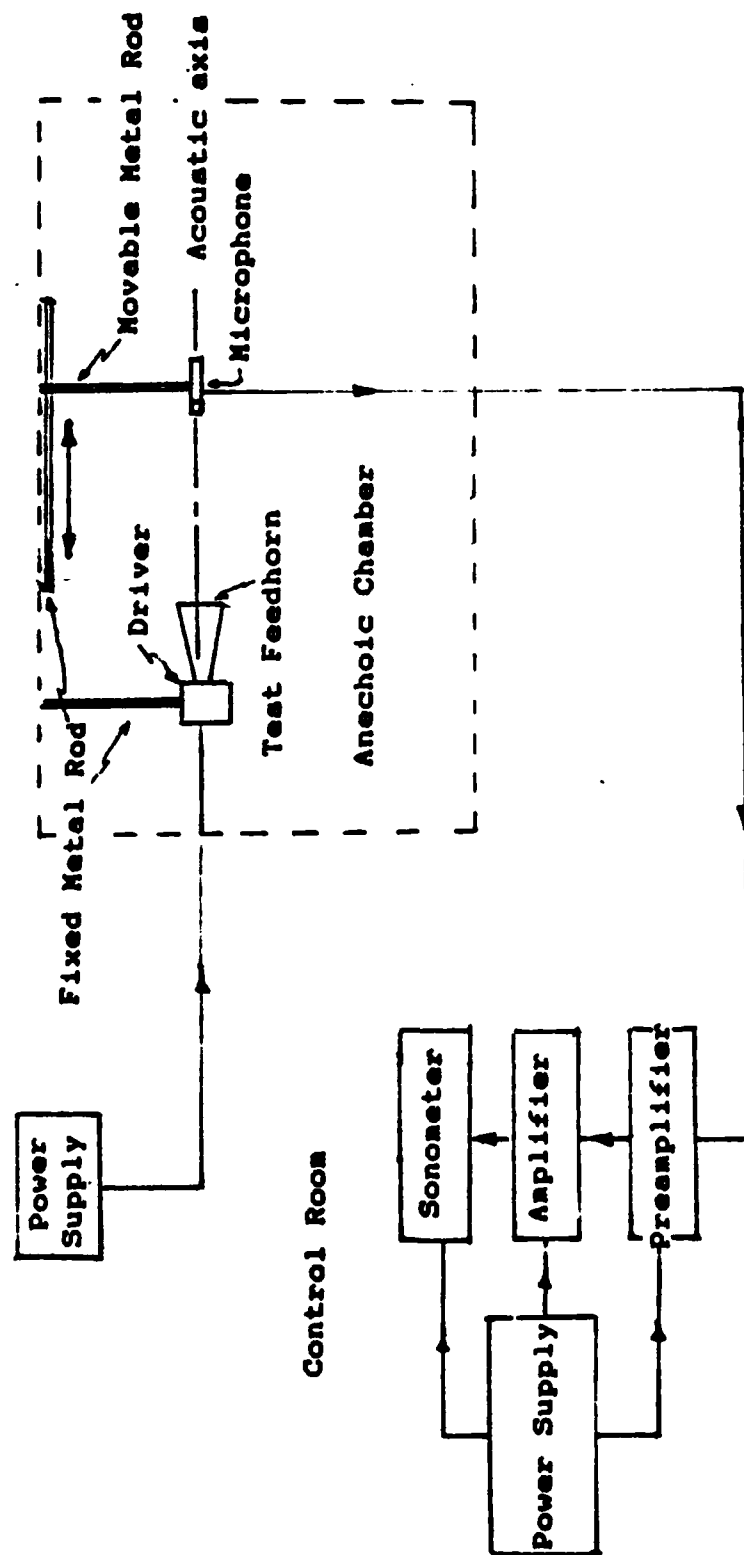


Figure 9. Intensity Level Testing Equipment Setup

transducer, as with the power measurements, the microphone was fixed and the transducer/horn assembly was rotated. The calibrated microphone was suspended from a fixed bar attached to the ceiling of the anechoic chamber. The transducer is suspended in front of the microphone at the same height starting on the acoustic axis. The metal rod holding the transducer assembly was attached to a mechanically rotatable plate. The motor for the movable plate was run from the control room of the chamber. The microphone, fixed at a one meter distance from the driver face and driven from a separate power supply, was connected to the sonometer and voltmeter. From a potentiometer on the plate, an angular output was read. This output, as well as the intensity level output from the sonometer, are coupled into an x-y plotter to produce a direct hardcopy voltage/angular beam pattern. Figure 10 shows the details of this setup.

3. Procedure

The acoustic pressure amplitude readings for each test feedhorn, as well as the driver itself, were made with the driver power amplifier set to feed a 1.6 kilohertz signal to the driver. The voltage to the eight ohm driver was maintained at one volt peak amplitude on the incoming signal. This level was a continuous wave and provided usable signals without overdriving the sensitive microphone. Since linear distance measurements along the

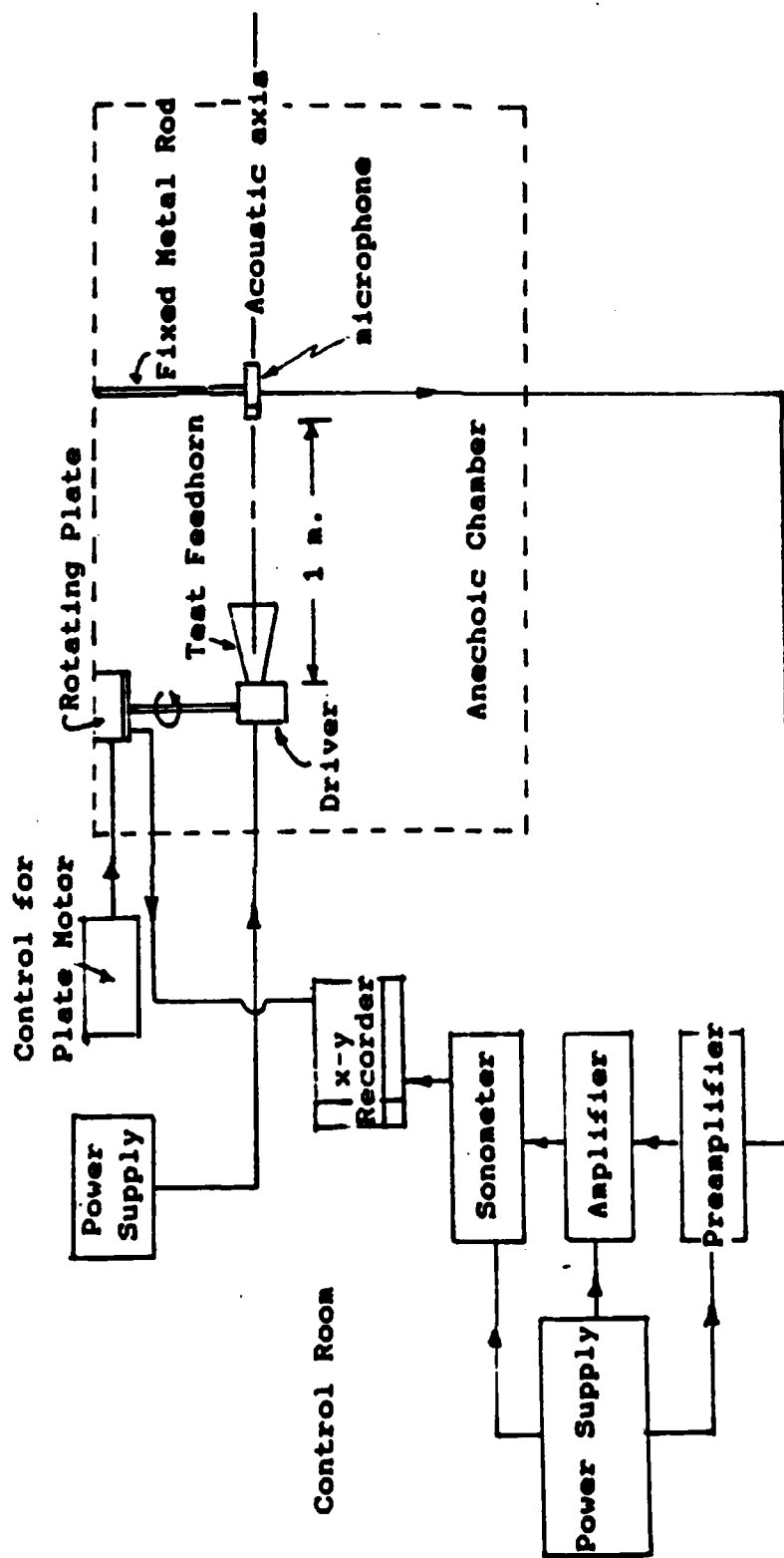


Figure 10. Beam Pattern Testing Equipment Setup

acoustic axis were difficult, if not impossible, to measure from the diaphragm itself it was determined that the easiest way to derive an accurate measurement was to make all distance readings from a plane incident to the mouth of each horn. The sonometer and amplifiers were run from 110 vac current. The reference intensity level for all readings was the standard atmospheric 10^{-12} watt/meter². Measurements were taken starting at one meter from the mouth of each test horn decreasing at ten centimeter increments until a plane incident with the horn was reached.

To get an accurate antenna beam pattern for each horn the driver was fed the same 1.6 kilohertz, 1 volt peak amplitude signal. The microphone was positioned at a fixed one meter distance from the driver face. Each horn was attached to the driver mounted on the movable plate. The sweep rate of the plate was set to coincide with 10 degrees of arc for every one half inch on the x axis of the graph and fed to the x input of the x-y recorder. The sonometer/amplifier system provided the y axis input to the x-y recorder. The acoustic axis of the horn was determined by sweeping the driver through several degrees of arc and watching for the maximum intensity level reading on the sonometer. Once centerline was determined the horn driver systems were rotated through 360 degrees and a beam pattern was obtained for each horn.

B. RESULTS

From the data obtained during the intensity measurements, it was clear the new designs were not as efficient as the theory predicted, but that the catenoidal design was a clear improvement over the conical horn. The peak intensity of the conical horn at the one meter point was -8.0 dB while the peak intensity of the exponential horn was a disappointing -13.8 dB. A partial explanation for the low efficiency may lie in the fact that the throat size of the exponential horn was designed to match the throat size of the conical horn. This throat size, 1.27 centimeters, does not take full advantage of the driver's 1.8 centimeter available aperture. The coupling of the horn to the driver may have been another source of low efficiency. Unless exact rigid mating of horn to driver face occurs, the overpressure caused by the sound wave propagation will leak through the irregularities of the interface. This problem was corrected in the catenoidal horn by placement of a rubber interface or gasket between the flange and driver face and securely anchoring it to the driver casing. The exponential horn fabrication process however provided some valuable information in the preparation of the catenoidal horn. Working with the exponential aluminum mold and getting the fiberglass to release from it was a difficult problem that was eventually solved only by the cutting of the shell and remating after the mold was removed. Of course, the seam

where the cut was made had to be delicately repaired. Any deviations in the inner face of the horn could cause reflections or interfering sound waves and reduce efficiency. The need for a gasket interface to prevent leakage was probably the most important lesson gained from the exponential design.

The catenoidal design proved much better, raising the intensity level to -1.1 dB at the one meter point. This is about a five fold increase in intensity for the catenoidal design over the conical horn. The catenoidal design takes full advantage of the larger opening in the driver and was designed with a 1.8 cm. throat diameter rather than the 1.27 cm. throat diameter of the conical and exponential designs. It also contains the rubber gasket that prevents a leak at the driver-horn interface.

To obtain the acoustic center for each horn, a graph was constructed plotting the inverse square root of the intensity against the distance. Since intensity is known to decrease with the inverse square root of the distance in the far field [Ref.6], these graphs can predict the point where the intensity approaches zero. This x intercept on the graph is the acoustic center of the horn. The graphs, which appear as Figures 11 through 13, show that the acoustic center of the conical design is 8 centimeters from the driver face. The exponential horn has an acoustic center 18.5 centimeters from the driver face and the catenoidal horn has an acoustic center 9.5 centimeters from the acoustic face.

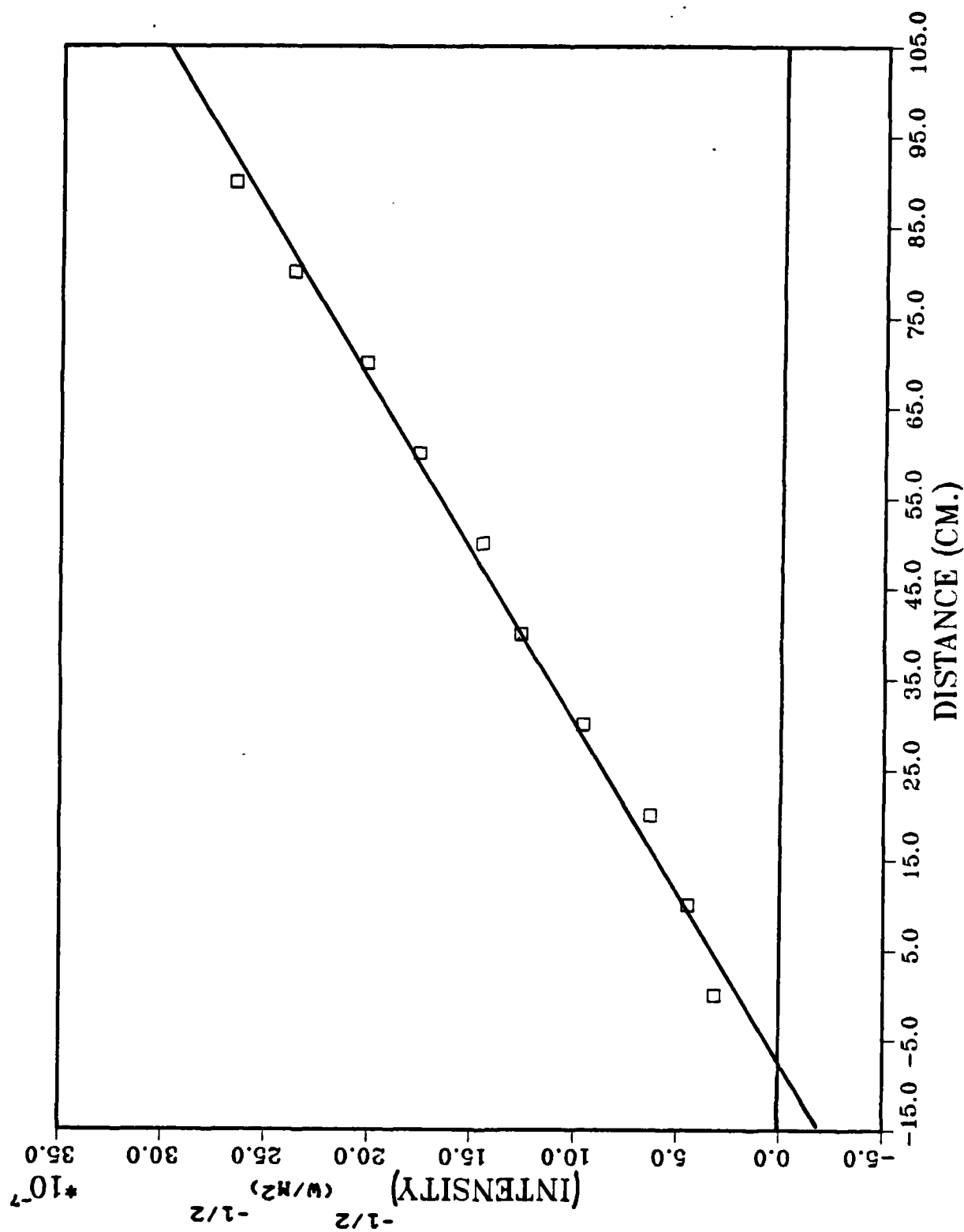


Figure 11. Graph of the Reciprocal of the Square Root of Intensity
versus Distance for the Conical Horn.

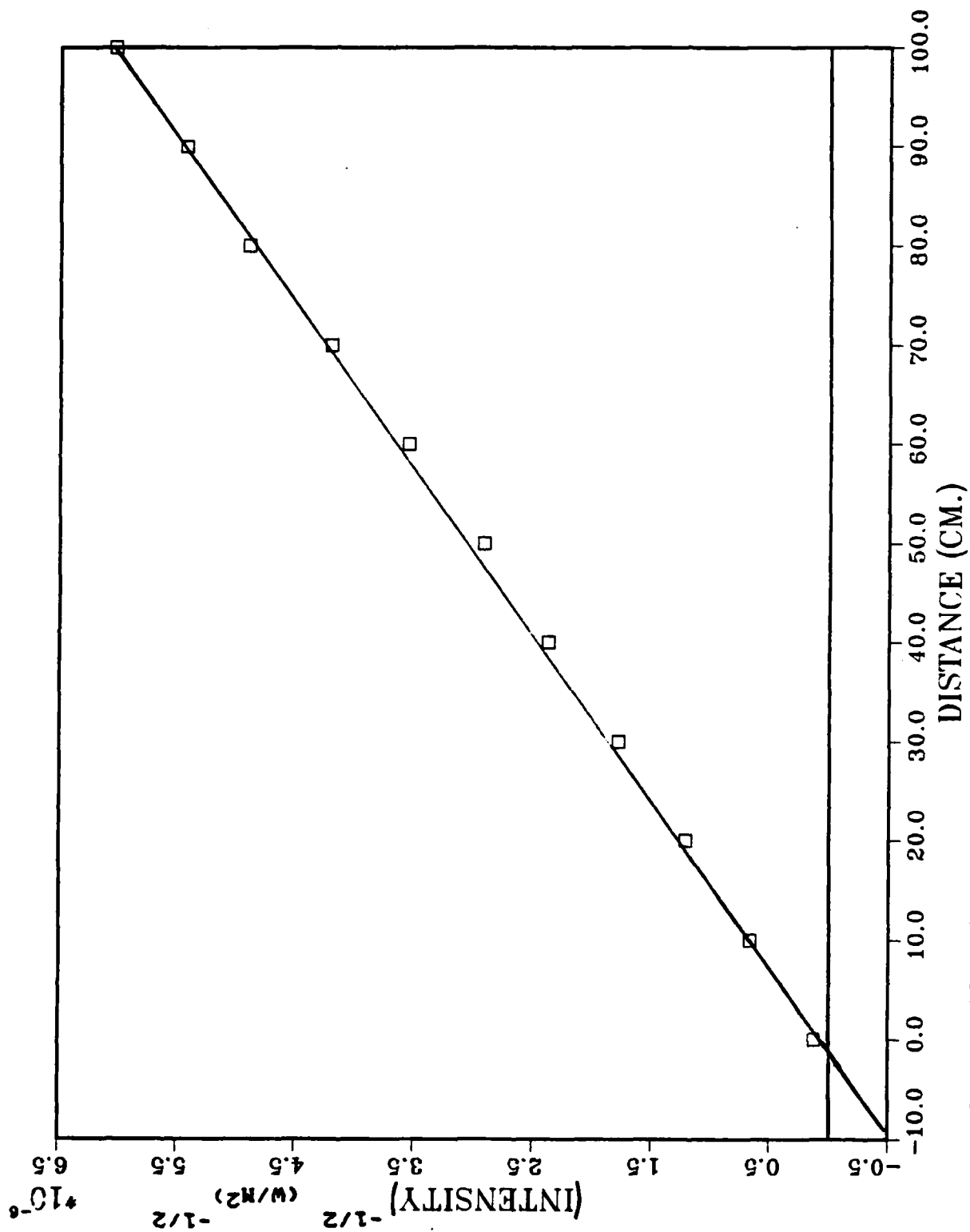


Figure 12. Graph of the Reciprocal of the Square Root of Intensity versus Distance for the Exponential Horn.

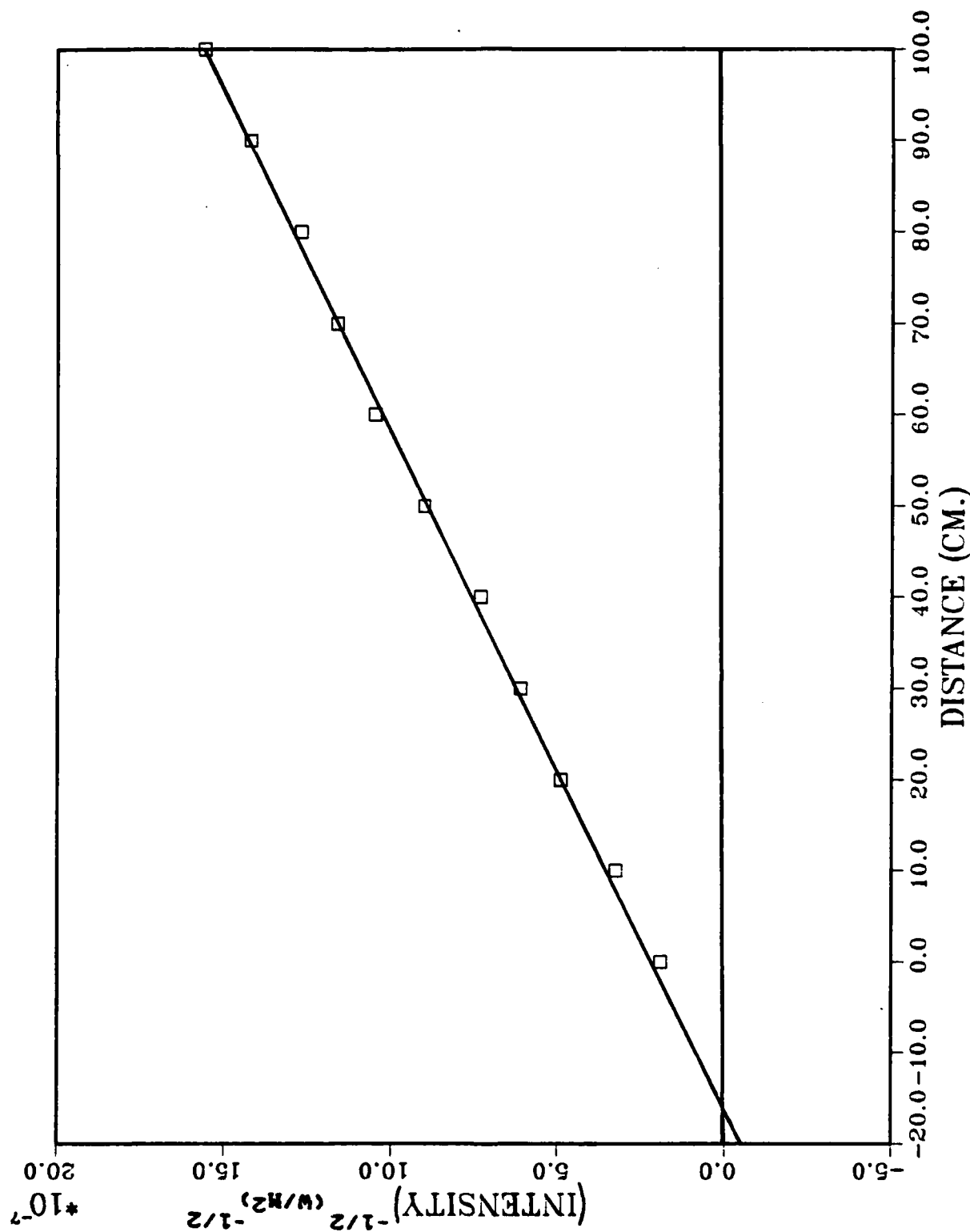


Figure 13. Graph of the Reciprocal of the Square Root of Intensity versus Distance for the Catenoidal Horn.

The beam patterns, which appear as Figures 14 through 17, provide some interesting results. The conical beam pattern (Fig. 14) shows two small side lobes at 40 degrees on either side of the central peak. These sidelobes peak at less than 15 percent of the mainlobe amplitude. In contrast the side lobes on the exponential and conical designs (Figs. 15 and 16) show more pronounced peaks in the same angular region. These sidelobes peak at 25 to 40 percent of the main lobe. Clearly this is undesirable [Ref. 7], but is a trade-off of the improved designs.

C. CONCLUSIONS AND RECOMMENDATIONS

The replacement of the conical horn with a high efficiency catenoidal design was the ultimate goal of this thesis. Theoretical transmission factors suggested that both an exponential and catenoidal horn should have about eight times the efficiency of the conical horn. A thirty percent decrease in intensity was observed in testing the exponential horn. This was attributable to the side leakage of the pressure wave by the improper mating of the horn to the driver face. Another explanation is that the exponential design did not take full advantage of the available 1.8 cm. driver aperture. The catenoidal horn had an intensity increase of 5 compared to the conical horn although a factor of 8 was expected. Considering the difficulty of

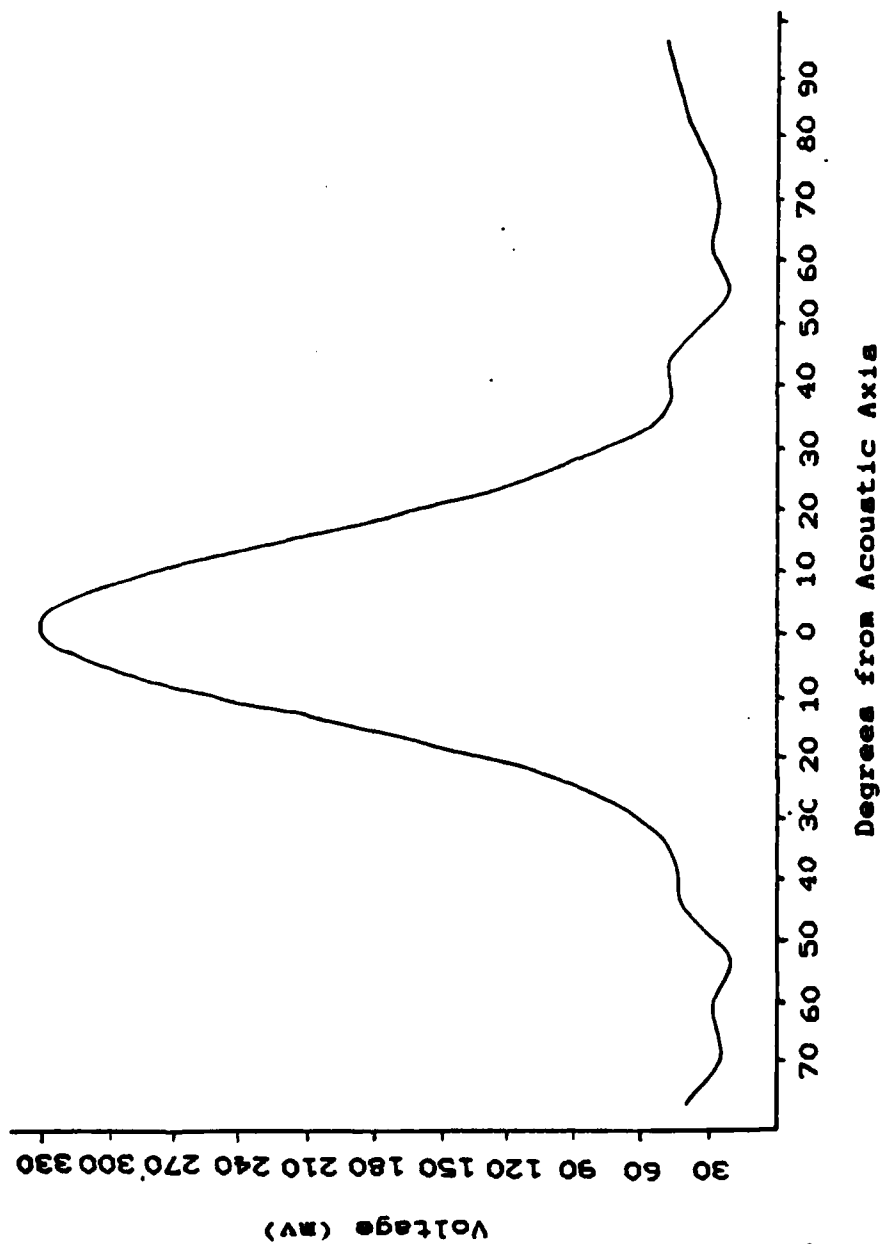


Figure 14. Beam Pattern of the Conical Horn at 1 Meter.

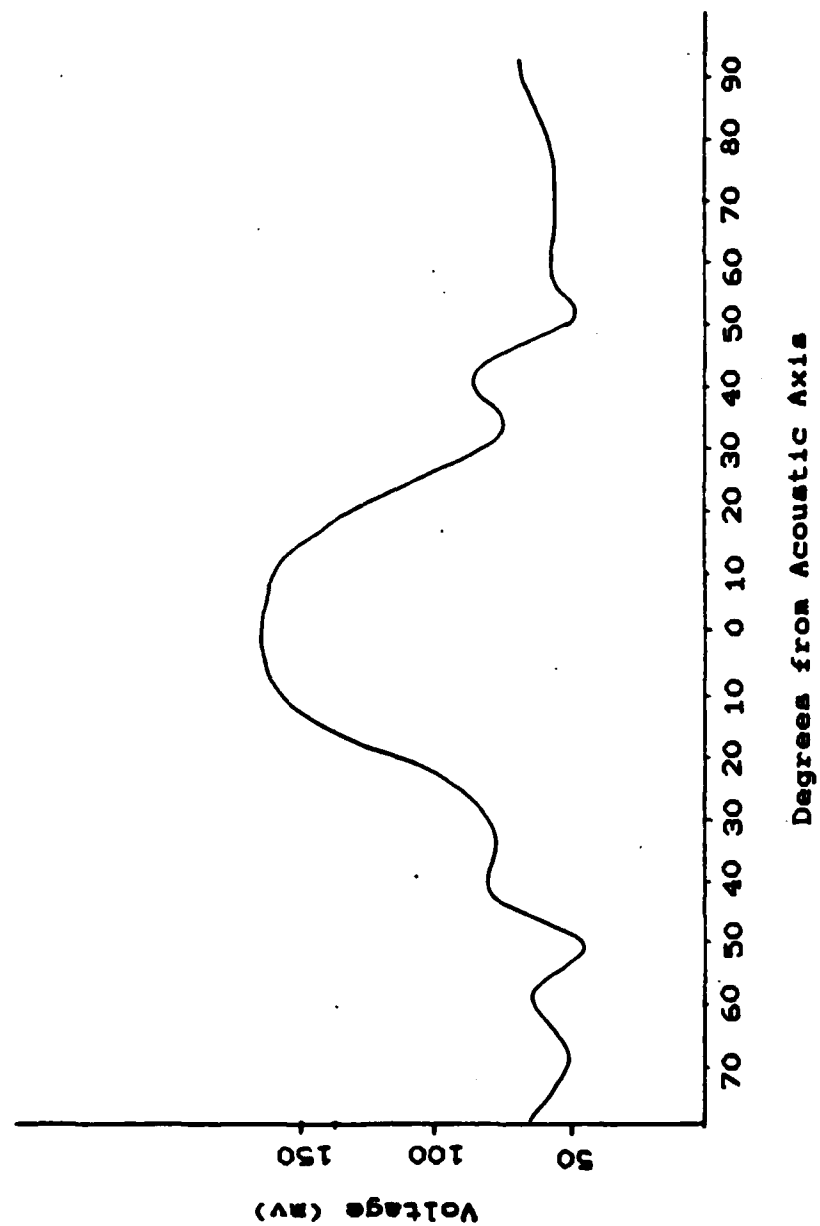


Figure 15. Beam Pattern of the Exponential Horn at 1 Meter.

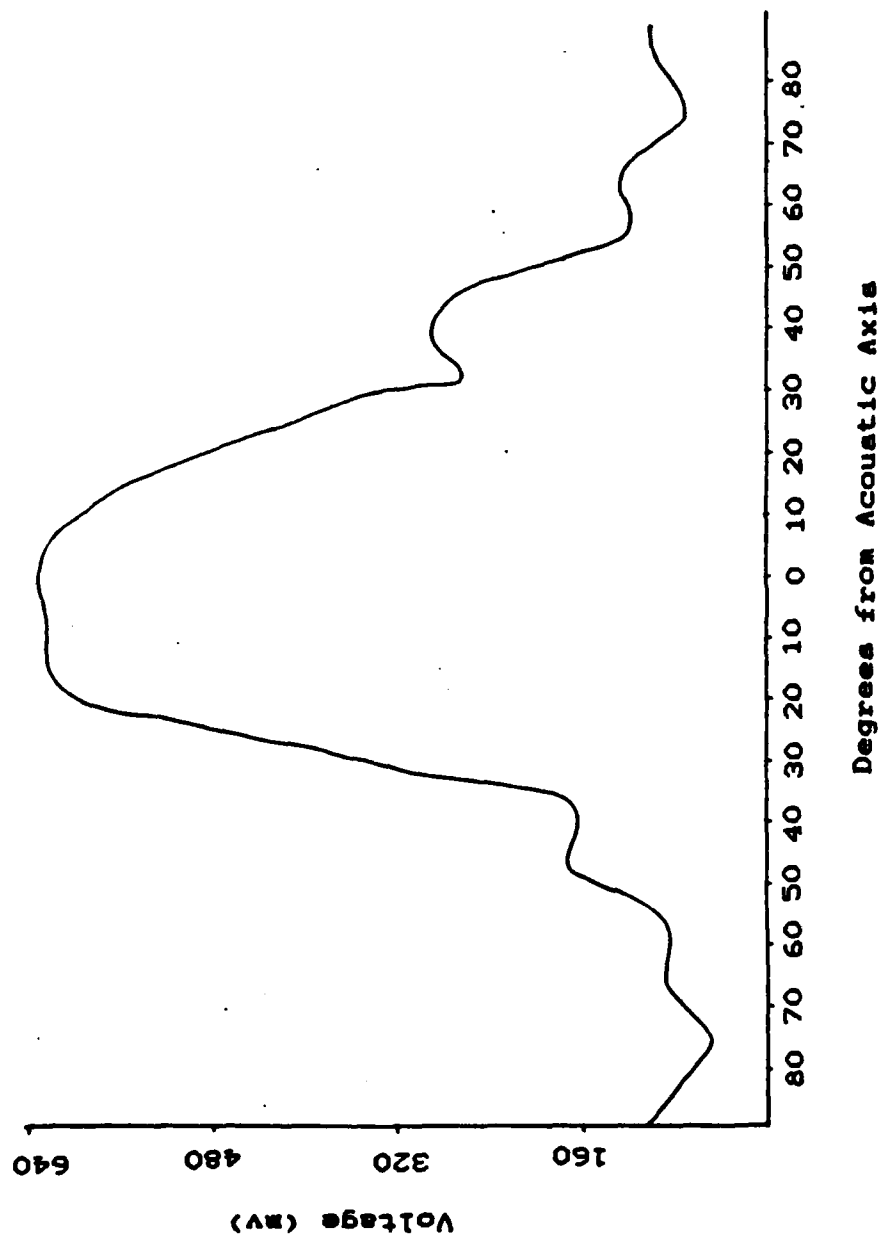


Figure 16. Beam Pattern of the Catenoidal Horn at 1 Meter.

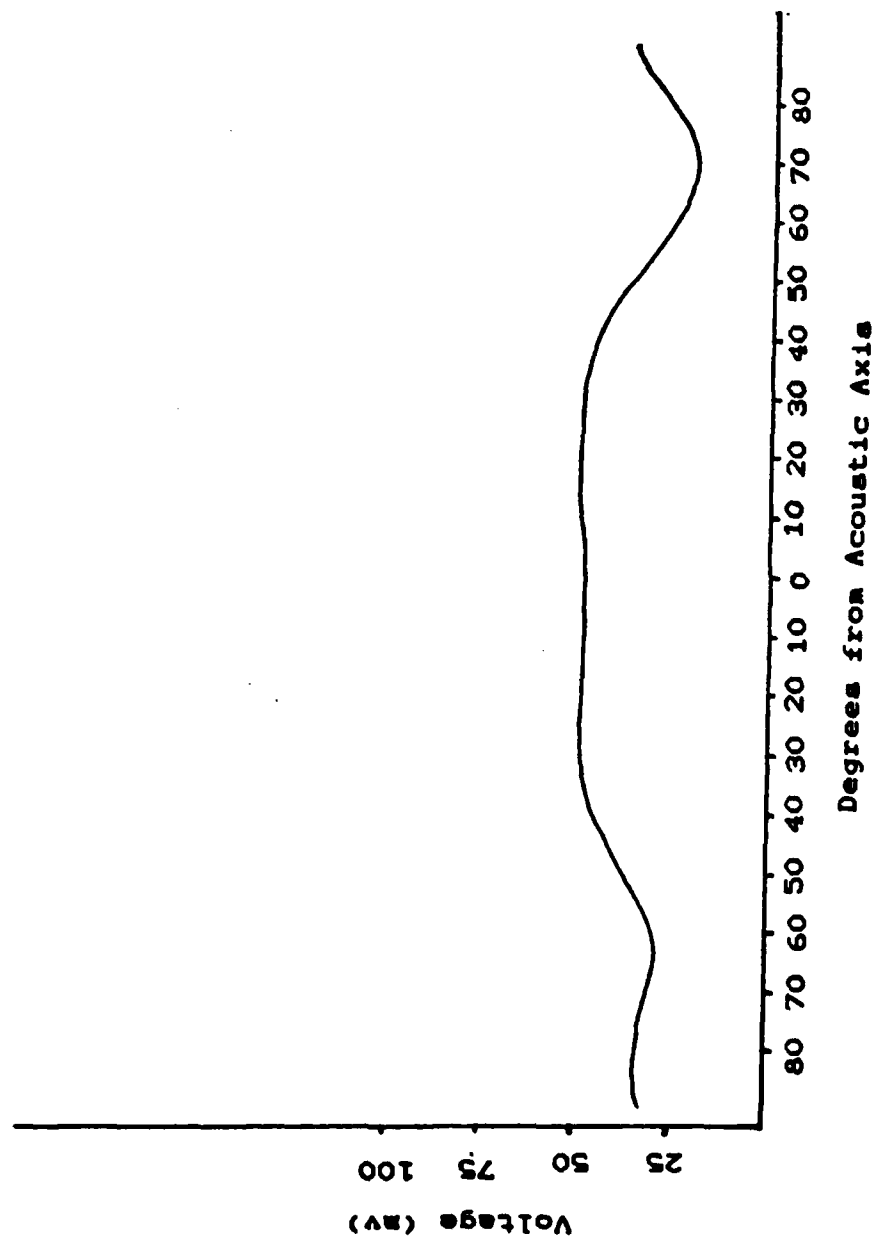


Figure 17. Beam Pattern of the Driver at 1 Meter.

manufacturing a smooth catenoidal horn from fiberglass, and the simplicity of the one dimensional horn theory, the measured improvement is in good agreement with the theory.

Even with the larger sidelobes discovered by beam pattern analysis, the catenoidal horn is recommended to replace the existing conical design. The five fold increase in output intensity is surely reason enough to use the upgraded design. The significant increase of intensity should extend the useable range of the sounder if the sidelobes can be adequately suppressed by the acoustic enclosure and will provide a important step in improving the range of the sounder.

APPENDIX A

DESIGN COMPUTER PROGRAMS

Exponential Design (Note: Language is Applesoft Basic)

```

10 REM INITIALIZE VARIABLES
20 LET SO=0; REM THROAT CROSSECTIONAL AREA
30 LET M=0; REM EXPONENTIAL FLARE CONSTANT
40 LET X=0; REM VARIABLE DISTANCE FROM THE THROAT
50 LET S=0; REM CROSSECTIONAL AREA AT ANY DISTANCE X
60 LET R=0; REM VARIABLE RADIUS
70 LET C=0; REM VARIABLE CIRCUMFERENCE
80 REM PRINT COLUMN HEADS
90 PRINT "X (M)";HTAB 6;"S (M^2)";HTAB 8;"RADIUS & CIRCUM. (M)"
100 VTAB 2
110 REM LOOP TO INCREMENT ALONG THE AXIS AT 1 CENTIMETER
120 REM INTERVALS TO A THIRTY CENTIMETER LENGTH
130 FOR X = .01 TO .31 STEP .01
140 LET SO=1.27E-4
150 LET M=18.98
160 LET S = SO * EXP(M * X)
170 LET R = SQR(S / 3.1416)
180 LET C = 2 * R * 3.1416
190 REM PRINT RESULTS
200 PRINT X;HTAB 3;PRINT S;HTAB 5;PRINT R;HTAB 5;PRINT C
210 NEXT X
220 END

```

Catenoidal Design

```

10 REM INITIALIZE VARIABLES
20 LET X=0; REM VARIABLE DISTANCE FROM THROAT
30 LET SO=0; REM THROAT CROSSECTIONAL AREA
40 LET H=0; REM CATENOIDAL FLARE CONSTANT
50 LET S=0; REM CROSSECTIONAL AREA AT ANY X
60 LET R=0; REM VARIABLE RADIUS
70 LET C=0; REM VARIABLE CIRCUMFERENCE
80 REM PRINT COLUMN HEADS
90 PRINT "X (M)";HTAB 6;"S (M^2)";HTAB 8;"RADIUS & CIRCUM. (M)"
100 VTAB 2
110 REM LOOP TO INCREMENT ALONG THE AXIS AT 1 CENTIMETER
120 REM INTERVALS TO A THIRTY CENTIMETER LENGTH
130 FOR X = .01 TO .31 STEP .01
140 LET SO=2.544E-4
150 LET H=0.1054
160 LET S=SO * (0.5 * (EXP (X/H) + EXP (-X/H))^2)

```



```
170 LET R= SQR(S/3.1416)
180 LET C= 2 * 3.1416 * R
190 REM PRINT RESULTS
200 PRINT X; HTAB 3;PRINT S;HTAB 5;PRINT R;HTAB 5;PRINT C
210 NEXT X
220 END
```

APPENDIX B

DIMENSIONS OF THE DESIGN HORNS

Exponential Design:

<u>Centimeters</u> <u>fm. Base</u>	<u>Inside</u> <u>Diameter</u>
0.0	1.27
1.0	1.40
2.0	1.54
3.0	1.69
4.0	1.86
5.0	2.04
6.0	2.24
7.0	2.47
8.0	2.72
9.0	2.99
10.0	3.23
11.0	3.61
12.0	3.97
13.0	4.37
14.0	4.80
15.0	5.28
16.0	5.80
17.0	6.38
18.0	7.02
19.0	7.72
20.0	8.48

Catenoidal Design:

<u>Centimeters</u> <u>fm. Base</u>	<u>Inside</u> <u>Diameter</u>
0.0	1.80
1.0	1.81
2.0	1.83
3.0	1.87
4.0	1.93
5.0	2.00
6.0	2.08
7.0	2.21
8.0	2.34
9.0	2.50
10.0	2.67
11.0	2.87
12.0	3.10
13.0	3.35
14.0	3.64
15.0	3.95
16.0	4.30
17.0	4.69
18.0	5.13
19.0	5.61
20.0	6.14
21.0	6.72
22.0	7.37
23.0	8.08
24.0	8.86
25.0	9.72

APPENDIX C

DATA

Note: All distances measured from mouth of horn.

Conical Horn:

<u>Distance (cm)</u>	<u>Intensity Level (dB)</u>	<u>Voltage (mv)</u>
100.0	-10.8	243
90.0	- 8.5	290
94.4	- 8.0	310
80.0	- 7.5	330
70.0	- 6.1	380
60.0	- 4.9	440
50.0	- 3.2	530
40.0	- 2.0	620
30.0	- 0.6	830
20.0	4.0	1200
10.0	7.0	1800
0.0	10.0	2200

Exponential Horn:

<u>Distance (cm)</u>	<u>Intensity Level (dB)</u>	<u>Voltage (mv)</u>
100.0	-15.4	133
90.0	-14.7	145
80.0	-13.8	160
70.0	-12.5	185
60.0	-11.0	220
50.0	- 9.3	268
40.0	- 7.5	330
30.0	- 5.0	435
20.0	- 1.7	641
10.0	3.5	1180
0.0	18.2	6200

Catenoidal Horn:

<u>Distance (cm)</u>	<u>Intensity Level (dB)</u>	<u>Voltage (mv)</u>
100.0	- 3.9	503
90.0	- 3.0	547
80.0	- 2.1	630
75.0	- 1.7	675
70.0	- 1.3	700
60.0	- 0.5	780
50.0	0.0	820
40.0	2.0	1005
30.0	4.3	1305
20.0	6.2	1690
10.0	9.8	2100
0.0	14.4	4800

Driver (no horn attached):

<u>Distance (cm)</u>	<u>Intensity Level (dB)</u>	<u>Voltage (mv)</u>
100.0	-24.9	45.0
90.0	-23.0	52.0
80.0	-21.9	62.5
70.0	-20.8	71.0
60.0	-19.7	80.8
50.0	-18.5	92.0
40.0	-16.0	120.0
30.0	-13.2	169.0
20.0	-10.0	246.0
10.0	- 4.0	500.0
01.0	19.2	7200.0

LIST OF REFERENCES

1. Acoustic Radar Manual, 2nd ed., pp. 1-7, Aerovironment Inc., 1975.
2. Merhaut, J., Theory of Electroacoustics, pp. 182-203, McGraw-Hill, 1981.
3. Morse, P. M., Vibration and Sound, pp. 265-281, Acoustical Society of America, 1976.
4. Ibid., pp. 282-283.
5. Beranek, L. L., Acoustics, pp. 259-268, McGraw-Hill, 1954.
6. Kinsler, L. E. and others, Fundamentals of Acoustics, p. 116, Wiley, 1982.
7. Olsen, H. F., Elements of Acoustical Engineering, pp. 184-193, Nostrand, 1947.

INITIAL DISTRIBUTION LIST

	No. Copies
1. Defense Technical Information Center Cameron Station Alexandria, Virginia 22304-6145	2
2. Library, Code 0142 Naval Postgraduate School Monterey, California 93943-5100	2
3. Professor D. L. Walters, Code <u>61 We</u> Department of Physics Naval Postgraduate School Monterey, California 93943-5100	4
4. Professor E. A. Milne, Code <u>61 Mn</u> Department of Physics Naval Postgraduate School Monterey, California 93943-5100	2
5. LT W. L. Richards, USN 29 Iroquois Dr. Pittsburgh, Pennsylvania 15205	2

END

FILMED

11-85

DTIC